Pseudo-phosphorylation of essential light chains affects the functioning of skeletal muscle myosin

Daria S. Yampolskaya[a], Galina V. Kopylova[b], Daniil V. Shchepkin[b], Salavat R. Nabiev[b], Larisa V. Nikitina[b], Jonathan Walklate[c], Rustam H. Ziganshin[d], Sergey Y. Bershitsky[b], Michael A. Geeves[c], Alexander M. Matyushenko[a], Dmitrii I. Levitsky[a,*]

[a] *Bach Institute of Biochemistry, Research Center of Biotechnology of the Russian Academy of Sciences, Leninsky prosp. 33, Moscow 119071, Russia*

[b] *Institute of Immunology and Physiology of the Russian Academy of Sciences, Yekaterinburg, 620049, Russia*

[c] *School of Biosciences, University of Kent, Canterbury CT2 7NJ, United Kingdom.*

[d] *Shemyakin-Ovchinnikov Institute of Bioorganic Chemistry of the Russian Academy of Sciences, ul. Miklukho-Maklaya 16/10, Moscow 117997, Russia*

Abbreviations: ELC, essential light chain; S1, myosin subfragment 1; LC1, light chain 1 of myosin from fast skeletal muscle

* Corresponding author.

E-mail address: Levitsky@inbi.ras.ru (D.I. Levitsky)

ABSTRACT

The work aimed to investigate how the phosphorylation of the myosin essential light chain of fast skeletal myosin (LC1) affects the functional properties of the myosin molecule. Using mass-spectrometry, we revealed phosphorylated peptides of LC1 in myosin from different fast skeletal muscles. Mutations S193D and T65D that mimic natural phosphorylation of LC1 were produced, and their effects on functional properties of the entire myosin molecule and isolated myosin head (S1) were studied. We have shown that T65D mutation drastically decreased the sliding velocity of thin filaments in an *in vitro* motility assay and strongly increased the duration of actin-myosin interaction in optical trap experiments. These effects of T65D mutation in LC1 observed only with the whole myosin but not with S1 were prevented by double T65D/S193D mutation. The T65D and T65D/S193D mutations increased actin-activated ATPase activity of S1 and decreased ADP affinity for the actin-S1 complex. The results indicate that pseudo-phosphorylation of LC1 differently affects the properties of the whole myosin molecule and its isolated head. Also, the results show that phosphorylation of LC1 of skeletal myosin could be one more mechanism of regulation of actin-myosin interaction that needs further investigation.

Keywords:
Myosin
Essential light chain
Pseudo-phosphorylation
Actin-myosin interaction
Mechanism of muscle contraction

1. Introduction

The molecular mechanism of muscle contraction is based on the cyclic interaction of myosin heads with actin filaments and is accompanied by ATP hydrolysis in the heads. The molecules of all types of muscle myosin consist of two heavy and four light chains. The N-terminal parts of heavy chains form globular heads capable of performing the motor function [1, 2]. The myosin head, or subfragment 1 (S1), consists of two major structural domains, the motor and the regulatory ones. The regulatory domain corresponds to a long α-helix, stabilized by two light chains, the essential light chain (ELC) and the regulatory light chain (RLC) [3]. The functioning of the myosin head involves a rotation of the regulatory domain (lever arm) relative to the motor domain during the ATPase cycle [2, 4, 5]. This rotation is accompanied by an interaction between the motor domain and ELC [6–8].

Both RLC and ELC can undergo phosphorylation. In skeletal and cardiac muscles, RLC is phosphorylated by Ca^{2+}/calmodulin-dependent myosin light chain kinase (MLCK). The phosphorylation alters myosin structure and function and enhances the Ca^{2+}-sensitivity and muscle contractility [9–11]. Much less is known about ELC phosphorylation, and no specific kinase, responsible for ELC phosphorylation, has been identified yet.

For the first time, ELC phosphorylation was discovered in 2001 by proteomic analysis of rabbit ventricular myocytes [12]. Using mass spectrometry, the authors identified two phosphorylation sites in the ventricular ELC corresponding to Thr65 and Ser193 of ELC (LC1) from human fast skeletal muscle, i.e., the sites highly conserved among various ELCs [12]. The degree of rabbit ventricular ELC phosphorylation was estimated to be ~26%, including 21% of monophosphorylated ELC and 5% of ELC phosphorylated at both sites.

Along with evidence of naturally occurring ELC phosphorylation, works showing its physiological significance have appeared. Important results have been obtained on zebrafish *Danio rerio* with a nonsense mutation in the gene encoding ventricular ELC that leads to ELC expression truncated at C-terminus [13]. Such mutant zebrafish ("lazy susan" mutant of ELC) lacks 11 amino acid residues at the ELC C-terminus, including phosphorylable Ser195. This mutation severely impaired cardiomyocyte contractility, whereas overexpression of WT ELC fully restored it. Importantly, overexpression of ELC carrying Ser195Ala substitution did not recover the contractile function. By contrast, the substitution of Ser195 by phosphomimetic Asp residue (Ser195Asp) restored the contractility. These results indicate the significance of the C-terminal phosphorylation of ELC Ser195 in the regulation of cardiac contractility *in vivo* [13]. The authors showed that the lack of this site decreased the sliding velocity of actin

filaments over ventricular myosin in the *in vitro* motility assay but did not affect the actin-activated ATPase activity of myosin [14].

The degree of ELC phosphorylation depends on physiological conditions. The physical stress of adult zebrafish significantly increased the degree of ELC phosphorylation mainly due to dual-phosphorylation at both sites, Thr66 and Ser195 [14]. It was shown that the treatment of cardiomyocytes with isoprenaline, which has a stimulating effect on the heart, increased the degree of ELC phosphorylation by 40% [15]. Treatment of ventricular cardiomyocytes with adenosine [16] increased the level of ELC phosphorylation from 26% to 34% [12]. It was suggested that phosphorylation of myosin ELC might become a new target for the modulation of cardiomyocyte contractility and to rescue the unfavorable effects of cardiomyopathy-causing mutations [14, 17, 18]. In particular, it was demonstrated that pseudo-phosphorylation of ELC by S195D substitution can efficiently rescue negative effects caused by cardiomyopathy-associated mutations A57G and M173V in ELC [18, 19].

It should be noted that till now all studies of ELC phosphorylation were only performed with cardiac ELC but nothing was known about the effects of phosphorylation of skeletal muscle ELC. Amino acid sequences of cardiac and skeletal ELC isoforms are highly conserved throughout known striated muscle ELC sequences of various animals, especially in the regions of proposed ELC phosphorylation sites (Ser193 and Thr65 in LC1 isoform of fast skeletal muscle) [12, 13]. This suggests that these sites can undergo phosphorylation not only in cardiac ELC but also in myosin ELC (LC1) of skeletal muscle.

The present work is focused on studying the role of LC1 phosphorylation in the functioning of skeletal myosin. Using mass spectrometry, we have searched phosphorylated peptides in the LC1 samples obtained from several fast skeletal muscles. We applied various methods to investigate how LC1 pseudo-phosphorylation affects the functional properties of the entire myosin molecule and isolated S1. For this purpose, we generated skeletal muscle ELC (LC1 isoform of fast skeletal muscle myosin) carrying mutations S193D or T65D that mimic LC1 phosphorylation at Ser193 or Thr65, respectively. The recombinant LC1 was introduced into skeletal myosin or S1 and their functional properties were characterized.

2. Materials and methods

All procedures involving animal care and handling were performed according to institutional guidelines set forth by the Animal Care and Use Committee at the Institute of Immunology

and Physiology Ural Branch of the Russian Academy of Sciences and Directive 2010/63/EU of the European Union.

2.1. Protein preparations

All ELC species used in this work were recombinant proteins containing the His-tag at the N-terminus. Human LC1 (the product of MYL1 gene, UniProt P05976) of fast skeletal muscle myosin, both wild type (WT) and T65D, S193D, and T65D/S193D mutants, were prepared in the bacterial expression plasmid pMW172 by PCR-mediated site-directed mutagenesis using Pfu DNA Polymerase (SibEnzyme, Novosibirsk, Russia). The following oligonucleotides were used for mutagenesis: 5'-GTTTGACAGAGATGGTGATTCCAAGA-3' for T65D, 3'-ATATAGGATCCTTAGAATCCATGATGTGCTT-5' for S193D, and both of them for T65D/S193D (mutant codons are underlined). The PCR products were cloned and sequenced to verify the substitutions. The constructs were used to transform the *E. coli* strain BL21(DE3)pLysS, large-scale cultures were grown and overexpression was induced according to standard methods [20]. The LC1 species were purified using affinity chromatography on a HisTrap HP 5 ml column (Amersham Pharmacia). The concentration of LC1 was determined spectrophotometrically using extinction coefficient $A^{1\%}$ at 280 nm of 2.0 cm^{-1}.

Rabbit skeletal muscle actin and myosin were prepared by established standard methods [21–22]. Actin filaments (F-actin) were polymerized by the addition of 4 mM $MgCl_2$ and 100 mM KCl to a monomeric G-actin solution. For an *in vitro* motility assay and optical trap experiments, F-actin was labeled with a 2-fold molar excess of TRITC-phalloidin (Sigma Chemical Co., St Louis, MO, USA), and for stopped-flow experiments, it was labeled with pyrene with N-(1-pyrenyl)iodoacetamide [23]. Myosin subfragment 1 (S1) was prepared by digestion of rabbit skeletal myosin filaments with TLCK-treated α-chymotrypsin (Sigma Chemical Co.) [24]. The concentration of S1 was estimated spectrophotometrically using extinction coefficient $A^{1\%}$ at 280 nm of 7.5 cm^{-1}.

2.2. Exchange of LC1 in myosin and S1

Recombinant WT LC1 and LC1 mutants T65D, S193D, and T65D/S193D were introduced into S1 according to the exchange procedure described by Zaager and Burke [25] with some modifications [7, 26]. Briefly, the exchange was performed by incubation of S1 with an 8-fold molar excess of free LC1 mutants in 50 mM imidazole-HCl buffer (pH 7.0)

containing 5 mM DTT, 10 mM MgATP, and 100 mM NaCl at 37°C for 30 min. The reaction was stopped by cooling on ice. S1 was purified on an SP-trisacryl column, using a linear gradient from 0 to 200 mM NaCl, to separate S1(LC1) from free LC1 [27]. After that, the S1 was purified by affinity chromatography on a HisTrap HP 1 ml column (50 mM Tris-HCl, pH 8.0, 300 mM NaCl), using a linear gradient from 15 to 500 mM imidazole, to obtain a preparation with completely exchanged LC1, since only the S1 molecules with His-tag on LC1 were held on this column. After dialysis against 20 mM Tris-HCl buffer (pH 8.0) containing 0.5 M NaCl and 2 mM $CaCl_2$ (or chromatography on NAP 20 column), the N-terminal His-Tag was removed from LC1 bound to S1 by cleavage with factor Xa protease (at Xa to S1 molar ratio 1:3) at 4°C overnight, and the reaction was stopped by PMSF. The output concentration of S1 with substituted LC1 was around 0.4 mg/ml.

To introduce recombinant LC1 species into myosin, we used the exchange procedure similar to that described for S1 with some modifications. First, the exchange was performed by incubation of myosin with LC1 species at higher ionic strength, 0.8 M NaCl, to prevent its aggregation. Then myosin was precipitated by dialysis against 50 mM Tris-HCl buffer, pH 8.0, containing 15 mM imidazole and 50 mM NaCl. After centrifugation of dialysate at 12,000 g, myosin precipitate was dissolved in the same buffer containing 0.8 M NaCl and purified by affinity chromatography on a 1 ml HisTrap HP column using a linear gradient of imidazole from 15 to 500 mM. As a result, a fraction of myosin molecules containing recombinant LC1 with N-terminal His tag in both heads was obtained, which released from the column at higher imidazole concentrations than the molecules with recombinant LC1s in only one of two heads and differed from other fractions by LC1 electrophoretic mobility studied by SDS–PAGE [28]. And finally, the N-terminal His-Tag was removed from LC1 bound with myosin heads by cleavage with factor Xa protease, as was described above for S1.

2.3. In vitro motility assay

Measurements of the sliding velocities of actin filaments were performed in the *in vitro* motility assay at 30 ^{o}C as described previously [29–32]. In brief, myosin (300 μg/ml) containing recombinant LC1 in both heads was loaded into an experimental flow cell with a nitrocellulose-coated inner surface. The sliding velocities of the filaments were measured in the presence of 2 mM ATP. The experiments with each myosin containing recombinant LC1 (either WT LC1 or LC1 mutants) in both heads were repeated three times, and velocity values were expressed as mean ± S.D.

2.4. Optical trap

Characteristics of single interactions of myosin (whole molecule) and S1 with F-actin were measured using a two-beam optical trap setup as described earlier [33–36]. The setup built on the base of an inverted fluorescent microscope (AxioObserver, Carl Zeiss Microscopy GmbH) enabled measurements of both step size *d* of a single myosin molecule or S1 during its interaction with F-actin in displacement mode, and duration *t* of this interaction. The average duration was calculated as described by Knight *et al*. [37]. The measurements were performed in the presence of 10 μM ATP either with myosin containing recombinant LC1 in both heads or with S1 comprising recombinant LC1. The concentration of myosin or S1 added into the flow cell was 0.5–1 μg/ml.

The distributions of the step sizes of the molecule of whole myosin and S1 consisted of two data sets located symmetrically about zero, which we fitted by Gaussians (Supplementary Fig. S2). We determined the step size as corresponding to the peak position of the bigger Gaussian, assuming it is correctly oriented to the polarity of the actin filament (See Supplementary materials for more detail).

2.5. Stopped-flow experiments

Rapid kinetic stopped-flow experiments were carried out at 20 ^{o}C with a standard Hi-Tech SF-61 DX2 stopped-flow spectrophotometer. For these experiments, actin was labeled with pyrene as described [23]. The pyrene fluorescence was excited at 365 nm. Experimental buffer contained 20 mM MOPS, 25 mM KCl, 5 mM $MgCl_2$, and 1 mM NaN_3 (pH 7.0). The concentrations used to describe the experimental conditions in the text are the final concentrations established after mixing the reactants in the stopped-flow (dilution by 2, 1:1 mixing). The final concentrations of S1 and F-actin were both 0.5 μM. Final ADP concentration varied from 0 mM to 4 mM for the 7 measurements of the multiple stopped-flow experiments, in which the amplitude of changes of the pyrene fluorescence decreased with increasing ADP concentration after mixing with 10 μM Mg-ATP. The ADP dissociation constant K_{AD} (μM), representing the affinity of ADP for the actin-S1 complex and defining the ADP inhibition of the ATP-induced dissociation of the complex, was calculated from observed rate constants k_{obs} (s^{-1}) for the ATP-induced acto-S1 dissociation reaction as described earlier [38].

2.6. ATPase measurements

Conventional methods used for measurements of the S1 ATPase activity usually need a relatively high S1 concentration that was virtually unacceptable for S1 comprising recombinant LC1. Therefore in the present study, we used the luciferin-luciferase system to investigate an actin-activated Mg^{2+}-dependent ATPase activity of S1 with recombinant LC1. We used Sigma-Aldrich #L-0633 set, a mixture of luciferin and luciferase, destined to detect picomolar concentrations of ATP. Samples contained 5 mM imidazole (pH 7.0), 10 mM $MgCl_2$, 87 nM S1, and 4.7 μM F-actin. The ATPase reaction was initiated by the addition of 10 mM ATP. As far as luciferase itself cleaves ATP and so may contribute to the reaction kinetics, the only time of luminescence quenching was used as a parameter of the ATPase rate. Measurement of the luminescence decrease was carried out by PerkinElmer Multimode Plate Reader (PerkinElmer, Waltham, MA, USA). Luminescence emission was monitored at 560 nm and 20 °C.

2.7. Mass spectrometry

Sample preparations. Mass spectrometry was used to search phosphorylated peptides in LC1 samples obtained from rabbit skeletal muscle myosin. For this purpose, small pieces (250 mg) were taken from various rabbit skeletal muscles (*m. psoas major*, *m. quadriceps femoris, m. latissimus dorsi,* and *m. erector spinae*), immediately frozen in liquid nitrogen, and stored at –80°C. Myosin was prepared from these samples according to the standard procedure [22] with the only exception that at all stages the buffer contained 10 mM EDTA, 10 mM Na pyrophosphate, 20 mM Na_3VO_4, 20 mM NaF, and 30 mM β-mercaptoethanol to prevent dephosphorylation of light chains. Myosin samples were subjected to SDS–PAGE [28], after that electrophoretic strips corresponding to LC1 were cut out from the gel and subjected to in-gel digestion of LC1 with endoproteinase Glu-C from *Staphylococcus aureus* V8 in phosphate buffer pH 7.8, which was performed as described previously for in-gel digestion of proteins with trypsin for mass spectrometric analysis [39].

Liquid chromatography and mass spectrometry (LC-MS/MS). The LC-MS/MS experiments were performed as described earlier [40] with some changes. Briefly, reverse-phase chromatography was performed with an Ultimate 3000 Nano LC System (Thermo Fisher Scientific), which was coupled to the Orbitrap Tribrid Lumos mass spectrometer (Thermo Fisher Scientific) via a nanoelectrospray source (Thermo Fisher Scientific).

Data analysis. Mass spectrometry raw files were analyzed by PEAKS studio 10.0 (Bioinformatics Solutions Inc.) [41] and peak lists were searched against the

Oryctolagus_cuniculus (rabbit) in Uniprot-SwissProt FASTA database version of 11.2021 (894 entries) with a deamidation Asn/Gln, Met oxidation and Ser/Thr/Tyr phosphorylation as variable modifications. Enzyme specificity in the database search was set to an endoproteinase Glu-C from *Staphylococcus aureus* V8 in phosphate buffer (digest mode – semispecific), and a maximum of three missed cleavages were allowed in the database search. The false discovery rate was set to 0.01 for peptide-spectrum matches and was determined by searching a reverse database. Peptide identification was performed with an allowed initial precursor mass deviation up to 10 p.p.m. and an allowed fragment mass deviation of 0.02 Da.

3. Results

3.1. Mass-spectrometry analysis of LC1 peptide fragments

We applied mass-spectrometry (LC-MS/MS) to search for phosphorylated residues in LC1 samples from various rabbit skeletal muscles (see Materials and methods for more details). Data are available via ProteomeXchange with the identifier PXD032361 (DOI**:** 10.6019/PXD032361). Phosphorylated peptide fragment 56-AFLL**Y**DR**T**GD**S**KI**T**L**S**QVGDVLRALG**T**NP**T**NAE-88 was revealed among peptides obtained from the LC1 sequence of *m. psoas major*, *m. quadriceps femoris*, and *m. erector spinae.* This fragment contained 7 potentially phosphorylable Ser, Thr, or Tyr residues (shown in bold): Tyr60, Thr63, peptide **S**KI**T**L**S** (residues 66–71 in the amino acid sequence of rabbit skeletal LC1), Thr82, and Thr85. The Thr63 residue corresponds to the Thr65 residue of human skeletal LC1). Only one of these residues was phosphorylated in this peptide fragment as the 80 Da shift corresponding to the addition of a single phosphate moiety was observed. The Tyr59, Thr82, and Thr85 residues can be excluded because shortened but phosphorylated fragment 62-R**T**GD**S**KI**T**L**S**QVGDVLR-78 obtained from LC1 of *m. latissimus dorsi* did not contain these residues. Thus, only Thr63, as well as Ser66, Thr69, and Ser71 of the SKITLS peptide can be phosphorylated in skeletal LC1. The phosphorylated peptide fragments were identified by LC-MS/MS analysis with a high score (–10lgP) equal to 61.45 for LC1 from *m. psoas major*, 58.87 and 52.93 for LC1 from *m. quadriceps femoris*, 31.44 for LC1 from *m. latissimus dorsi,* and 68.47 for LC1 from *m. erector spinae*.

We have not found any phosphorylated Ser residues at LC1 C-terminus (namely, Ser191 in rabbit LC1 corresponding to Ser193 in human skeletal muscle LC1).

3.2. Sliding velocity of actin filaments in the in vitro motility assay: effect of the mutations mimicking phosphorylation of the LC1 in both myosin heads

We used the *in vitro* motility assay to investigate how mutations mimicking LC1 phosphorylation in both myosin heads affect the sliding velocity of F-actin over the whole myosin. The S193D mutation did not influence the sliding velocity of F-actin, whereas the T65D mutation drastically (by almost 2.5 times) decreased the velocity compared with WT LC1 (from 5.1 ± 0.5 μm/s to 2.1 ± 0.3 μm/s) (Fig. 1). Intriguingly, the sliding velocity of actin filaments over myosin with double mutation T65D/S193D in LC1 (4.1 ± 0.5 μm/s) was not appreciably different from that for myosin with WT LC1 and S193D LC1 (Fig. 1). Thus, the S193D mutation, which itself did not affect the sliding velocity of actin filaments, nevertheless prevented a dramatic effect of the T65D mutation.

We were unable to perform experiments with S1 after LC1 substitution most likely due to its concentration being too low for the *in vitro* motility assay; even at the maximum available S1 concentration of ~0.4 mg/ml, the filaments left still. (See Supplementary materials for more detail).

3.3. Unitary interactions of myosin heads with F-actin

Although the step size of S1 and the whole myosin molecule were the same, the interaction duration of S1 containing WT LC1 by more than 1.5 times exceeded that of myosin with WT LC1 (Table 1). A similar difference in the interaction duration was observed by Kad et al. [42] in smooth muscle, where the lifetime of attachment of S1 almost two times exceeded that of two-headed HMM (189 ms vs 104 ms, respectively).

All mutations that mimic LC1 phosphorylation did not affect the myosin step size (Table 1). As for the duration of the actin-myosin interaction, the T65D mutation in LC1 extended it by a factor of 5, while the S193D mutation by only 30% (Fig. 2A, Table 1). Surprisingly, the double T65D/S193D mutation increased the duration of interaction by only 2.5 times (Table 1), i.e., much weaker than the T65D mutation did. This result indicates that the S193D mutation suppresses the dramatic increase in the duration of the actin-myosin interaction caused by the T65D mutation.

Like in the case with the whole myosin molecule, the LC1 mutants did not affect the step size of S1 (Table 1). However, the effects of the mutations on the duration of the interaction of S1 and myosin with F-actin differed strikingly. The T65D mutation decreased

the duration of actin-S1 interaction by 25% (Fig. 2B, Table 1), whereas the S193D mutation in LC1 had no appreciable influence on the actin-S1 interaction duration, and the double mutation shortened it.

Thus, the results of these studies indicated that LC1 pseudo-phosphorylation differently affects the duration of the interaction of whole myosin and S1 with F-actin.

3.4. Effects of LC1 pseudo-phosphorylation on actin-activated ATPase activity of S1

We studied the actin-activated Mg^{2+}-dependent ATPase activity of S1 with recombinant LC1 using the luciferin-luciferase system. The luminescence intensity curves obtained for S1 samples, which reflected the decrease of the ATP content during the actin-activated ATPase reaction of S1, are presented in Fig. 3A. The T65D and double T65D/S193D mutations in LC1 increased the actin-activated ATPase activity of S1 (Fig. 3A). The time of the luminescence intensity decrease to zero was 32 ± 0.9 min for S1 with T65D mutation and 22.9 ± 0.7 min for S1 with double mutation T65D/S193D, while for S1 with WT LC1 it was 38.4 ± 1.1 min (mean ± SEM from 6-8 measurements) (Fig. 3B). The effect of a single S193D mutation in LC1 on the S1 ATPase activity was insignificant (Fig. 3A, B).

3.5. ATP-induced dissociation of acto-S1 complexes and its inhibition by ADP

The results presented above demonstrate that mutations mimicking LC1 phosphorylation affect the sliding velocity of F-actin over myosin in the *in vitro* motility assay (Fig. 1) and the actin-activated ATPase activity of S1 (Fig. 3). It was shown in previous studies that the sliding velocity of F-actin over myosin is about equivalent to the unloaded shortening velocity of a muscle fiber [43–45]. Both these velocities tightly correlate with the ADP affinity for actomyosin complex (K_{AD}) measured by defining the ADP inhibition of the ATP-induced dissociation of the complex [38, 46, 47]. It was also demonstrated that the ADP dissociation constant K_{AD} shows a good correlation with actomyosin ATPase activity [46]. Summing up these data, one can propose that the T65D and T65D/S193D mutations in LC1, which accelerate the ATPase activity of the acto-S1 complex (Fig. 3), should affect the K_{AD} value. Therefore in the present study, we investigated in stopped-flow experiments, how LC1 pseudo-phosphorylation affects the ADP dissociation constant, K_{AD}. For this, the rate constants k_{obs} (s^{-1}) for the ATP-induced acto-S1 dissociation were measured at different ADP concentrations (Fig. 4 and Supplementary Fig. S3). As [ADP] increased from zero to mM values the single exponential k_{obs} value for the dissociation reaction decreased. K_{AD} values for

acto-S1 complexes were calculated as described earlier [38]. The results showed that both the T65D and double T65D/S193D mutations caused a 1.5-fold increase in the K_{AD} value compared to S1 containing WT LC1 (Table 2).

4. Discussion

The goal of the work was to find out how ELC pseudo-phosphorylation can affect the functional properties of skeletal muscle myosin at the molecular level. All previous studies on ELC phosphorylation were performed only with cardiac ELC but nothing was known about the phosphorylation of skeletal muscle ELC and the effects that such modification may have on the properties of skeletal muscle myosin. Amino acid sequences of cardiac and skeletal ELC isoforms are highly conserved, particularly at phosphorylation sites (Thr64 and Ser195 in human ventricular ELC) [12]. This allows suggesting that sites Thr65 and Ser193 in LC1 of skeletal myosin can also undergo phosphorylation. We tested this assumption with mass-spectrometry and revealed phosphorylated peptides. Then we produced LC1 carrying mutations S193D or T65D that mimic LC1 phosphorylation at Ser193 or Thr65, respectively, and studied the properties of skeletal myosin or S1 containing those LC1s.

4.1. Does LC1 phosphorylation really occur in skeletal muscle myosin?

As known, amino acid sequences of cardiac and skeletal ELC isoforms are highly conserved throughout known striated muscle ELC sequences of various animals. Starting current work, we expected to find phosphorylable sites (Ser193 and Thr65) in the LC1 isoform of human fast skeletal muscle similar to those, which undergo phosphorylation in cardiac LC1 [12]. In rabbit fast skeletal myosin, these correspond to Ser191 and Thr63.

Using mass spectrometry (LC-MS/MS), we have analyzed peptide fragments from LC1 of fast rabbit skeletal myosin and discovered four potentially phosphorylable residues Ser and Thr in its N-terminal part: Thr63, Ser66, Tht69, or Ser71, corresponding to Thr65, Ser68, Thr71, and Ser73 in human skeletal LC1. It appeared that only one of them was phosphorylated. The result confirms that the N-terminal part of skeletal myosin LC1 can undergo phosphorylation like that in cardiac myosin.

In the LC1 C-terminal part, we were unable to find phosphorylated Ser residues, namely, Ser191 in rabbit LC1 corresponding to Ser193 in human skeletal muscle LC1. The reason could be that this residue on the flexible C-terminus of LC1 was simply lost upon LC1 proteolysis. Another explanation is that this residue, even being initially phosphorylated,

undergoes a rather fast dephosphorylation upon LC1 preparation, despite the use of inhibitors of phosphatase activity. This explanation can be supported, at least partly, by literature data showing that cardiac LC1 undergoes irreversible thiophosphorylation by myosin light chain kinase using ATPγS as a substrate, but no phosphate incorporation into LC1 could be observed upon reversible phosphorylation using ATP [48, 49].

The SKITLS peptide containing potentially phosphorylable Ser and Thr residues is present only in the amino acid sequence of LC1 from human and rabbit skeletal muscles, but not in the sequence of cardiac LC1 [12] (see Fig. 5). Previous studies were only performed with human cardiac ELC where highly conserved Thr64 residue was phosphorylated [12], and this prompted us to investigate the effects caused by pseudo-phosphorylation of Thr65 residue in human skeletal LC1. However, the mass-spectrometry indicated that not only Thr63 in rabbit skeletal LC1, corresponding Thr65 in human skeletal LC1, but also Ser and Thr residues in the SKITLS peptide can be phosphorylated.

In the crystal structure of rabbit skeletal myosin, phosphorylable residues of the SKITLS peptide are located near Thr63 within the region, which does not directly interact with the α-helix of the heavy chain in the myosin regulatory domain (Fig. 6). This region contains many negatively charged oxygen atoms including those in Thr63, Ser66, Thr69, and Ser71 residues, as well as in negatively charged Asp61 and Asp65 (Fig. 6B). The introduction of additional negative charges into this region by phosphorylation of Ser or Thr residues should lead to extra destabilization of this region due to electrostatic repulsion between the residues. In turn, this destabilization should change the LC1 structure and functional properties of myosin, which we did observe for myosin with LC1 pseudo-phosphorylated at Thr65 residue.

4.2. Effects of the T65D mutation

The T65D mutation in LC1 substantially changed the properties of skeletal myosin. With the whole myosin, this mutation drastically decreased the sliding velocity of F-actin in the *in vitro* motility assay (Fig. 1) and strongly increased the duration of unitary actin-myosin interaction (Fig. 2A, Table 1).

In general, an increase in the sliding velocity of F-actin, as well as the unloaded shortening velocity of a muscle fiber, correlate well with an increase in ADP dissociation constant K_{AD}, i.e., with a decrease in the ADP affinity [38, 46, 47]. In the case of S1, the T65D mutation decreased the ADP affinity for the acto-S1 complex (Table 2), and the

lifetime of its unitary complex with F-actin (Fig. 2B, Table 1), which agrees well with the rise of ATPase activity of the complex (Fig. 3).

The question arose why the effects of T65D mutation in LC1 are so different for myosin and S1? We believe this difference can be explained by cooperative interaction between the two heads of the myosin molecule, as was proposed by Marcus Schaub with colleagues long ago [50–53] and then confirmed by other authors [54–55]. In particular, a significant difference in the mechanical behavior between single- and double-headed skeletal myosin was shown in the optical-trap experiments [54]. Subsequently, a new state of myosin, the super relaxed state (SRX), with a very slow ATP turnover rate has been observed in skeletal muscle. This state, which was initially discovered in rabbit skeletal muscle by Roger Cooke with colleagues [56], was thereafter also seen in various skeletal and cardiac myosins [57–60]. It was shown that the SRX state is significantly stabilized by intramolecular head–head and head–tail interactions in myosin (so called "interacting-heads motif", IHM) [58–60]. This can explain the difference between S1 and the whole myosin in the interaction duration with actin (Table 1), which can result from the absence of IHM motif in S1 in contrast to the two-headed myosin molecule. It has recently been shown that cardiomyopathic mutations in ELC can stabilize or destabilize the SRX state of cardiac myosin [61]. It is possible that the T65D mutation in LC1 can affect the SRX state in myosin and modify it.

Another explanation is that the T65D mutation could influence the LC1 interaction with RLC. This interaction was shown to play an important role in the activation of myosin molecule by RLC phosphorylation in smooth muscle; in particular, disruption of the interplay between the RLC and ELC significantly diminishes the actin-activated ATPase of myosin with phosphorylated RLC and its ability to move actin filaments in the *in vitro* motility assay [62, 63]. One can propose that ELC-RLC interaction can also occur in cardiac and skeletal muscles. In favor of this assumption are recently published data showing that cardiomyopathy-causing mutations in ELC controlling the SRX state stability affect the phosphorylation of RLC in the heart muscle [61]. Our data point out the possibility of RLC-ELC interplay in skeletal myosin. However, it should be noted that this interaction in skeletal muscle myosin had not been demonstrated yet. We were unable to directly test the assumption concerning LC1-RLC interaction in skeletal myosin as S1 used in our study was prepared by chymotryptic digestion of myosin and so devoid of RLC.

4.3. Effects of the S193D mutation

The S193D mutation in LC1 had no appreciable influence on the myosin properties, it only increased slightly the duration of the actin-myosin interaction but not the actin-S1 interaction (Table 1), and caused a statistically insignificant effect on the actin-activated ATPase activity of S1 (Fig. 3). These results are in some contradiction with those obtained on cardiac myosin of zebrafish [13, 14], which indicated an important role of phosphorylation of the ELC C-terminal site in the regulation of cardiac contractility in vivo. However, our results showed that LC1 C-terminal phosphorylation in skeletal muscle is unlikely significantly affects the functional properties of myosin. The difference could be accounted for by the distinctions between heavy chains of cardiac and skeletal myosin.

4.4. Effects of double T65D/S193D mutation

In S1, the effects of the combined T65D/S193D mutation did not significantly differ from those of the T65D mutation. Like T65D, double T65D/S193D mutation decreased the lifetime of the unitary acto-S1 complex (Table 1) and reduced its affinity for ADP (Table 2). It also increased the actin-activated ATPase activity of S1, and this effect was more pronounced than for the T65D mutation (Fig. 3).

The most intriguing data were obtained for the whole myosin with the double T65D/S193D mutation in LC1. In this combination, the S193D mutation fully or partly prevented dramatic changes in functional properties of myosin caused by the T65D mutation (Fig. 1, Table 1). Importantly, this effect was observed only with the whole myosin but not with S1, which can be explained by the interaction between the two heads of the myosin molecule or the LC1-RLC interplay. In any case, it seems likely that the S193D mutation can restore normal functioning of the regulatory domain with associated LC1 and RLC (i.e., its rotation relative to the motor domain of the myosin head during the ATPase cycle), whose properties were significantly damaged by T65D mutation in LC1. One can propose that this situation may occur in skeletal muscle under some unfavorable conditions when phosphorylation of Thr65 or closely located Ser or Thr residues in LC1 can prevent excessive ATP consumption and phosphorylation of the C-terminal Ser residue suppresses this effect.

5. Conclusions

In the current work, we showed that LC1 in fast skeletal muscle undergoes phosphorylation and, for the first time, investigated how LC1 pseudo-phosphorylation affects the functional properties of skeletal muscle myosin. We found that pseudo-phosphorylation of

Thr65 dramatically changes the properties of the whole skeletal myosin and influences the characteristics of S1. Pseudo-phosphorylation of only Ser193 did not noticeably affect the functional properties of myosin. However, in the complex with T65D mutation, it suppressed the effects of the T65D. This observation suggests that phosphorylation of the C-terminal Ser residue can prevent the influence of the phosphorylation of Ser or Thr residues in the N-terminal part of LC1 of the whole myosin. As one can see, the data obtained on whole skeletal myosin and S1 do not coincide. The differences in the behavior between the whole myosin and S1 may serve as an argument for the cooperative interaction of the two heads of the myosin molecule.

We demonstrated that phosphorylation of LC1 of skeletal myosin could be one more mechanism of regulation of actin-myosin interaction and needs a deeper investigation.

Acknowledgments

This work was supported by State Program projects 122041100022-3 (to D.L.) and 122022200089-4 (to S.B.). The authors thank Dr. Oxana Gerzen for her help in the analysis of optical trap data.

Author contributions

D.S.Y., A.M.M., and D.I.L.: conceptualized the work, coordinated the study, and performed data curation; D.S.Y., G.V.K., D.V.S., S.Y.B., A.M.M., and D.I.L.: designed research; D.S.Y. and A.M.M.: prepared the LC1 mutants; D.S.Y.: performed ATPase experiments and analyzed data; G.V.K. and D.V.S.: performed *in vitro* motility experiments and analyzed data; S.R.N. and L.V.N.: performed optical trap experiments and analyzed data; J.W. and M.A.G.: performed stopped-flow experiments and analyzed data; R.H.Z.: performed mass spectrometry experiments and analyzed data; D.I.L., D.S.Y., G.V.K., D.V.S., M.A.G., S.Y.B., and A.M.M.: wrote the manuscript. All authors read and approved the manuscript.

Declaration of Competing Interest

The authors declare no conflict of interest.

References

[1] Y.Y. Toyoshima, S.J. Kron, E.M. McNully, K.R Niebling, C. Toyoshima, J.A. Spudich, Myosin subfragment-1 is sufficient to move actin filaments *in vitro*, Nature 328 (1987) 536–539.

[2] D.I. Levitsky, Actomyosin systems of biological motility, Biochemistry (Moscow) 69 (2004) 1177–1189.

[3] I. Rayment, W. Rypniewski, K. Schmidt-Base, R. Smith, D. Tomchick, M. Benning, D. Winkelmann, G. Wesenberg, H. Holden, Three-dimensional structure of myosin subfragment 1: a molecular motor, Science 261 (1993) 50–58.

[4] I. Rayment, The structural basis of the myosin ATPase activity, J. Biol. Chem. 271 (1996) 15850–15853.

[5] T.Q. Uyeda, P.D. Abramson, J.A. Spudich, The neck region of the myosin motor domain acts as a lever arm to generate movement, Proc. Natl. Acad. Sci. USA 93 (1996) 4459–4464.

[6] R. Dominguez, Y. Freyzon, K.M. Trybus, C. Cohen, Crystal structure of a vertebrate smooth muscle myosin motor domain and its complex with the essential light chain: visualization of the pre-power stroke state, Cell 94 (1998) 559–571.

[7] D.S. Logvinova, D.I. Markov, O.P. Nikolaeva, N.N. Sluchanko, D.S. Ushakov, D.I. Levitsky, Does interaction between the motor and regulatory domains of the myosin head occur during ATPase cycle? Evidence from thermal unfolding studies on myosin subfragment 1, PLoS One 10 (2015) e0137517.

[8] D.S. Logvinova, D.I. Levitsky, Essential light chains of myosin and their role in functioning of the myosin motor, Biochemistry (Moscow) 83 (2018) 944–960.

[9] J.S. Davis, S. Hassanzadeh, S. Winitsky, H. Lin, C. Satorius, R. Vemuri, A.H. Aletras, H. Wen, N.D. Epstein, The overall pattern of cardiac contraction depends on a spatial gradient of myosin regulatory light chain phosphorylation, Cell 107 (2001) 631–641.

[10] J.T. Stull, K.E. Kamm, R. Vandenboom, Myosin light chain kinase and the role of myosin light chain phosphorylation in skeletal muscle, Arch. Biochem. Biophys. 510 (2011) 120–128.

[11] K.E. Kamm, J.T. Stull, Signaling to myosin regulatory light chain in sarcomeres, J. Biol. Chem. 286 (2011) 9941–9947.

[12] D.R. Arrell, I. Neverova, H. Fraser, E. Marban, J.E. Van Eyk, Proteomic analysis of pharmacologically preconditioned cardiomyocytes reveals novel phosphorylation of myosin light chain 1, Circ. Res. 89 (2001) 480–487.

[13] B. Meder, C. Laufer, D. Hassel, S. Just, S. Marquart, B. Vogel, A. Hess, M.C. Fishman, H.A. Katus, W. Rottbauer, A single serine in the carboxyl terminus of cardiac essential myosin light chain-1 controls cardiomyocyte contractility in vivo, Circ. Res. 104 (2009) 650–659.

[14] L.M. Scheid, M. Mosqueira, S. Hein, M. Kossack, L. Juergensen, M. Mueller, B. Meder, R.H.A. Fink, H.A. Katus, D. Hassel, Essential light chain S195 phosphorylation is required for cardiac adaptation under physical stress, Cardiovasc. Res. 111 (2016) 44–55.

[15] S.C. Verduyn, R. Zaremba, J. van der Velden, G.J. Stienen, Effects of contractile protein phosphorylation on force development in permeabilized rat cardiac myocytes, Basic Res. Cardiol. 102 (2007) 476–487.

[16] H. Funaya, M. Kitakaze, K. Node, T. Minamino, K. Komamura, M. Hori, Plasma adenosine levels increase in patients with chronic heart failure, Circulation 95 (1997) 1363– 1365.

[17] D. Szczesna-Cordary, P.P. de Tombe, Myosin light chain phosphorylation, novel targets to repair a broken heart? Cardiovasc. Res. 111 (2016) 5–7.

[18] W. Huang, D. Szczesna-Cordary, Molecular mechanisms of cardiomyopathy phenotypes associated with myosin light chain mutations, J. Muscle Res. Cell Motil. 36 (2015) 433–445.

[19] W. Huang, Molecular mechanisms of myosin light chain mutation-induced cardiomyopathies, Open Access Dissertations (2015) Paper 1373.

[20] F.W.Studier, A.H. Rosenberg, J.J. Dunn, J.W. Dubendorff, Use of T7 RNA polymerase to direct expression of cloned genes, Methods Enzymol. 185 (1990) 60–89.

[21] J.D. Pardee, J.A. Spudich, Purification of muscle actin, Methods Enzymol. 85 (1982) 164–181.

[22] S.S. Margossian, S. Lowey, Preparation of myosin and its subfragments from rabbit skeletal muscle, Methods Enzymol. 85 (1982) 55–71.

[23] A.H. Criddle, M.A. Geeves, T. Jeffries, The use of actin labelled with N-(1-pyrenyl)iodoacetamide to study the interaction of actin with myosin subfragments and troponin/tropomyosin, Biochem. J. 232 (1985) 343–349.

[24] A.G. Weeds, R.S. Taylor, Separation of subfragment-1 isoenzymes from rabbit skeletal muscle myosin, Nature 257 (1975) 54–56.

[25] S. Zaager, M. Burke, Temperature and ionic strength dependence of the subunit interactions in vertebrate skeletal myosin. A comparison of the interaction between the alkali light and heavy chains of mammalian and avian myosin, J. Biol. Chem. 263 (1988) 13891–13895.

[26] D.S. Logvinova, A.M. Matyushenko, O.P. Nikolaeva, D.I. Levitsky, Transient interaction between the N-terminal extension of the essential light chain-1 and motor domain of the myosin head during the ATPase cycle, Biochem. Biophys. Res. Commun. 495 (2018) 163–167.

[27] H.R. Trayer, I.P. Trayer, Fluorescence resonance energy transfer within the complex formed by actin and myosin subfragment 1. Comparison between weakly and strongly attached states, Biochemistry 27 (1988) 5718–5727.

[28] U.K. Laemmli, Cleavage of structural proteins during the assembly of the head of bacteriophage T4, Nature 227 (1970) 680–685.

[29] A.M. Matyushenko, N.A. Koubassova, D.V. Shchepkin, G.V. Kopylova, S.R. Nabiev, L.V. Nikitina, S.Y. Bershitsky, D.I. Levitsky, A.K. Tsaturyan, The effects of cardiomyopathy-associated mutations in the head-to-tail overlap junction of α-tropomyosin on its properties and interaction with actin, Int. J. Biol. Macromol. 125 (2019) 1266–1274.

[30] A.M. Matyushenko, N.V. Artemova, D.V. Shchepkin, G.V. Kopylova, S.Y. Bershitsky, A.K. Tsaturyan, N.N. Sluchanko, D.I. Levitsky, Structural and functional effects of two stabilizing substitutions, D137L and G126R, in the middle part of α-tropomyosin molecule, FEBS J. 281 (2014) 2004–2016.

[31] A.M. Matyushenko, D.V. Shchepkin, G.V. Kopylova, S.Y. Bershitsky, N.A. Koubassova, A.K. Tsaturyan, D.I. Levitsky, Functional role of the core gap in the middle part of tropomyosin, FEBS J. 285 (2018) 871–886.

[32] A.M. Matyushenko, V.V. Nefedova, D.V. Shchepkin, G.V. Kopylova, V.Y. Berg, A.V. Pivovarova, S.Y. Kleymenov, S.Y. Bershitsky, D.I. Levitsky, Mechanisms of disturbance of the contractile function of slow skeletal muscles induced by myopathic mutations in the tropomyosin TPM3 gene, FASEB J. 34 (2020) 13507–13520.

[33] S.R. Nabiev, D.A. Ovsyannikov, A.K. Tsaturyan, S.Y. Bershitsky, The lifetime of the actomyosin complex in vitro under load corresponding to stretch of contracting muscle, Eur. Biophys. J. 44 (2015) 457–463.

[34] S.R. Nabiev, D.A. Ovsyannikov, G.V. Kopylova, D.V. Shchepkin, A.M. Matyushenko, N.A. Koubassova, D.I. Levitsky, A.K. Tsaturyan, S.Y. Bershitsky, Stabilizing of the central part of tropomyosin increases bending stiffness of thin filament, Biophys. J. 109 (2015) 373–379.

[35] D.V. Shchepkin, S.R. Nabiev, G.V. Kopylova, A.M. Matyushenko, D.I. Levitsky, S.Y. Bershitsky, A.K. Tsaturyan, Cooperativity of myosin interaction with thin filaments is enhanced by stabilizing substitutions in tropomyosin, J. Muscle Res. Cell Motil. 38 (2017) 183–191.

[36] L.V. Nikitina, G.V. Kopylova, D.V. Shchepkin, S.R. Nabiev, S.Y. Bershitsky, Study of molecular mechanisms of actin-myosin interaction in the heart muscle. Biochemistry (Moscow) 80 (2015) 1748–1763.

[37] A.E. Knight, C. Veigel, C. Chambers, J.E. Molloy, Analysis of single-molecule mechanical recordings: application to acto-myosin interactions, Prog. Biophys. Mol. Biol. 77 (2001) 45–72.

[38] M. Nyitrai, R. Rossi, N. Adamek, M.A. Pellegrino, R. Bottinelli, M.A. Geeves, What limits the velocity of fast-skeletal muscle contraction in mammals? J. Mol. Biol. 355 (2006) 432–442.

[39] A. Shevchenko, H. Tomas, J. Havlis, J.V. Olsen, M. Mann, In-gel digestion for mass spectrometric characterization of proteins and proteomes, Nature protocols 1 (2006) 2856–2860.

[40] E.V. Kryukova, C.A. Vulfius, R.H. Ziganshin, T.V. Andreeva, V.G. Starkov, V.I. Tsetlin, Y.N. Utkin, Snake C-type lectin-like proteins inhibit nicotinic acetylcholine receptors, J. Venom Res. 10 (2020) 23–29.

[41] B. Ma, K. Zhang, C. Hendrie, C. Liang, M, Li, A. Doherty-Kirby, G. Lajoie, PEAKS: powerful software for peptide de novo sequencing by tandem mass spectrometry, Rapid Commun. Mass Spectrom. 17 (2003) 2337–2342.

[42] N.M. Kad, A.S. Rovner, P.M. Fagnant, P.B. Joel, G.G. Kennedy, J.B. Patlak, D.M. Warshaw, K.M. Trybus, A mutant heterodimeric myosin with one inactive head generates maximal displacement, J. Cell Biol. 162 (2003) 481–488.

[43] M.A. Pellegrino, M. Canepari, R. Rossi, G. D'Antona, C. Reggiani, R. Bottinelli, Orthologous myosin isoforms and scaling of shortening velocity with body size in mouse, rat, rabbit and human muscles, J. Physiol. 546 (2003) 677–689.

[44] J. Walklate, C. Ferrantini, C.A. Johnson, C. Tesi, C. Poggesi,·M.A. Geeves, Alpha and beta myosin isoforms and human atrial and ventricular contraction, Cell. Mol. Life Sci. 78 (2021)7309–7337.

[45] C.D. Vera, C.A. Johnson, J. Walklate, A. Adhikari, M. Svicevic, S.M. Mijailovich, A.C. Combs, S.J. Langer, R.M. Ruppel, J.A. Spudich, M.A. Geeves, L.A. Leinwand, Myosin motor domains carrying mutations implicated in early or late onset hypertrophic cardiomyopathy have similar properties, J. Biol. Chem. 294 (2019) 17451–17462.

[46] S. Weiss, R. Rossi, M.A. Pellegrino, R. Bottinelli, M.A. Geeves, Differing ADP release rates from myosin heavy chain isoforms define the shortening velocity of skeletal muscle fibers, J. Biol. Chem. 276 (2001) 45902–45908.

[47] C.A. Johnson, J.E. McGreig, S.T. Jeanfavre, J. Walklate, C.D. Vera, M. Farré, D.P. Mulvihill, A.J. Baines, M. Ridout, L.A. Leinwand, M.N. Wass, M.A. Geeves, Identification of sequence changes in myosin II that adjust muscle contraction velocity, PLoS Biol. 19 (2021) e3001248. doi: 10.1371/journal.pbio.3001248.

[48] C. Bialojan, I. Morano, J.C. Ruegg, Different phosphorylation patterns of cardiac myosin light chains using ATP and ATPγS as substrates, J. Mol. Cell Cardiol. 20 (1988):575–578.

[49] I. Morano, J. Rosch, A. Arner, J.C. Ruegg, Phosphorylation and thiophosphorylation by myosin light chain kinase: different effects on mechanical properties of chemically skinned ventricular fibers from the pig, J. Mol. Cell Cardiol. 22 (1990) 805–813.

[50] M.C. Schaub, J.G. Watterson, P.G. Waser, Cooperation between the two myosin heads interacting with actin in the presence of ADP in myofibrils, Experientia 29 (1973) 316–318.

[51] M.C. Schaub, J.G. Watterson, P.G. Waser, Evidence for head-head interactions in myosin from cardiac and skeletal muscles, Basic Res. Cardiol. 72 (1977) 124–132.

[52] P.A. Kunz, K. Loth, J.G. Watterson, M.C. Schaub, Nucleotide induced head-head interaction in myosin, J. Muscle Res. Cell Motil. 1 (1980) 15–30.

[53] M.C. Schaub, J.G. Watterson, Symmetry and asymmetry in the contractile protein myosin, Biochimie 63 (1981) 291–299.

[54] M.J. Tyska, D.E. Dupuis, W.H. Guilford, J.B. Patlak, G.S. Waller, K.M. Trybus, D.M. Warshaw, S. Lowey, Two heads of myosin are better than one for generating force and motion, Proc. Natl. Acad. Sci. USA 96 (1999) 4402–4407. doi:10.1073/pnas.96.8.4402

[55] N. Albet-Torres, M.J. Bloemink, T. Barman, R. Candau, K. Froölander, M.A. Geeves, et al., Drug effect unveils inter-head cooperativity and strain-dependent ADP release in fast skeletal actomyosin, J. Biol. Chem. 284 (2009) 22926–22937. doi: 10.1074/jbc.M109.019232

[56] M.A. Stewart, K. Franks-Skiba, S. Chen, R. Cooke, Myosin ATP turnover rate is a mechanism involved in thermogenesis in resting skeletal muscle fibers, Proc. Natl. Acad. Sci. USA 107 (2010) 430–435.

[57] P. Hooijman, M.A. Stewart, R. Cooke, A new state of cardiac myosin with very slow ATP turnover: a potential cardioprotective mechanism in the heart, Biophys J. 100 (2011) 1969–1976. doi: 10.1016/j.bpj.2011.02.061.

[58] J.A. Rohde, O. Roopnarine, D.D. Thomas, J.M. Muretta, Mavacamten stabilizes an autoinhibited state of two-headed cardiac myosin, Proc. Natl. Acad. Sci. USA. 115 (2018) E7486–E7494. https://doi.org/10.1073/pnas.1720342115

[59] S. Chu, J.M. Muretta, D.D. Thomas, Direct detection of the myosin super-relaxed state and interacting-heads motif in solution, J. Biol. Chem. 297 (2021) 101157. https://doi.org/10.1016/j.jbc.2021.101157

[60] R. Craig, R. Padrón, Structural basis of the super- and hyper-relaxed states of myosin II, J. Gen. Physiol. 154 (2021) e202113012. https://doi.org/10.1085/jgp.202113012

[61] Y.H. Sitbon, F. Diaz, K. Kazmierczak, J. Liang, M. Wangpaichitr, D. Szczesna-Cordary, Cardiomyopathic mutations in essential light chain reveal mechanisms regulating the super-relaxed state of myosin, J. Gen. Physiol. 153 (2021) e202012801. https://doi.org/10.1085/jgp.202012801

[62] S. Ni, F. Hong, B.D. Haldeman, J.E. Baker, K.C. Facemyer, C.R. Cremo, Modification of interface between regulatory and essential light chains hampers phosphorylation-dependent activation of smooth muscle myosin, J. Biol. Chem. 287 (2012) 22068–22079.

[63] K.A. Taylor, M. Feig, C.L.Brooks 3rd, P.M. Fagnant, S. Lowey, K.M. Trybus, Role of the essential light chain in the activation of smooth muscle myosin by regulatory light chain phosphorylation, J. Struct. Biol. 185 (2014) 375–382.

Table 1

Parameters of single interactions of myosin or isolated myosin head (myosin subfragment 1, S1) containing WT LC1 or T65D, S193D, or T65D/S193D LC1 mutants with F-actin measured by the optical trap

LC1	Myosin		Myosin head (S1)	
	d (nm)	*t (ms)*	*d (nm)*	*t (ms)*
WT LC1	12.7 ± 3.4 (773)	16.7 ± 1.0	9.5 ± 4.1 (1009)	26.5 ± 0.4
T65D LC1	12.5 ± 3.2 (1535)	83.2 ± 9.9*	11.4 ± 3.8 (643)	19.7 ± 0.6*
S193D LC1	14.0 ± 3.1 (720)	22.7 ± 1.0*	11.7 ± 3.4 (599)	28.3 ± 1.8
T65D/S193D LC1	11.8 ± 3.5 (1356)	41.3 ± 2.8*	8.2 ± 2.9 (609)	19.3 ± 1.3*

d – Myosin step size (mean ± SD), *t* – duration of myosin interaction with F-actin filament (mean ± SEM). The number of analyzed events is shown in brackets. The comparisons were performed by the Student *t*-test. The * symbol denotes significant differences in the duration of interaction with F-actin for myosin or S1 containing LC1 with studied mutations from myosin or S1 with WT LC1 ($p < 0.05$).

Table 2

Effects of LC1 pseudo-phosphorylation by mutations T65D, S193D, or T65D/S193D on the ADP dissociation constant K_{AD} (μM) representing the affinity of ADP for the actin-S1 complex and defining the ADP inhibition of the ATP-induced dissociation of the complex.

LC1	**Average K_{AD} (μM)** (mean ± SEM)*
WT LC1	240.5 ± 9.5
T65D LC1	379.0 ± 3.0*
S193D LC1	176.5 ± 29.5
T65D/S193D LC1	354.5 ± 1.5*

*The average K_{AD} values were calculated from 5 measurements of rate constants k_{obs} (s^{-1}) observed at various ADP concentrations in 3 independent experiments.

Figure legends

Fig. 1. Sliding velocities of actin filaments over myosin containing recombinant LC1 in both heads (either WT LC1 or T65D, S193D, or T65D/S193D LC1 mutants) measured in the *in vitro* motility assay. The velocities are presented as mean ± S.D. for three experiments. The comparisons were performed by the Student *t*-test. The * symbol denotes a significant difference in the sliding velocity of the filaments over myosin containing LC1 with T65D mutation from that over myosin with WT LC1, $p < 0.05$.

Fig. 2. Frequency histograms obtained in the optical trap experiments and showing the distribution of duration of the interaction with F-actin of myosin (A) and isolated myosin heads (S1) (B) containing either WT LC1 or LC1 with T65D mutation. Solid lines (for WT LC1) and dashed lines (for T65D LC1) are exponential fits to the duration distributions. For average values of the duration of single interaction see Table 1.

Fig. 3. A). Representative curves showing effects of LC1 mutations T65D, S193D, and T65D/S193D on the actin-activated S1 ATPase measured using the luciferin-luciferase system. The ATPase reaction was initiated by the addition of 10 mM ATP.
B). Average time at which a decrease in the luminescence intensity occurs for S1 containing WT LC1 and LC1 mutants T65D, S193D, or T65D/S193D. The time values are presented as mean ± SEM from 6–8 measurements. The comparisons were performed by the Student *t*-test. The symbol (*) denotes significant differences in the time value for S1 containing LC1 T65D and T65D/S193D mutants from S1 with WT LC1 ($p < 0.0001$).

Fig. 4. Representative plots showing the ADP dependence of rate constants k_{obs} (s^{-1}) for the ATP-induced dissociation of acto-S1 complex formed by S1 containing WT LC1 (A) and LC1 mutants T65D (B), S193D (C), or T65D/S193D (D). Final ADP concentrations established after mixing the reactants in the stopped-flow are shown.

Fig. 5. Alignment of internal amino acid sequences of myosin LC1 from various sources encompassing proposed phosphorylation sites: rabbit skeletal LC1 (P02602), human skeletal LC1 (P05976), and human ventricular LC1 (P08590). The sequences were from the UniProtKB database. Phosphorylated Thr residue identified by mass spectrometry in human ventricular LC1 is shown in bold, potentially phosphorylable Ser and Thr residues in rabbit skeletal LC1 are shown in italic, and Thr65 residue in human skeletal LC1, which was

pseudo-phosphorylated by mutation T65D in this work is underlined. Identical (*) amino acid residues and conserved (**:**) or semi-conserved (**.**) substitutions are indicated below the aligned sequences. Numbers before and after sequences indicate the amino acid position of the first and last amino acid, respectively.

Fig. 6. A) Crystal structure of rabbit skeletal muscle LC1 (beige) associated with α-helix of the heavy chain (crimson) in the regulatory domain of the myosin head (PDB: 6YSY).
B) Enlarged and turned LC1 region containing potentially phosphorylable Thr63, Ser66, Thr69, and Ser71 residues (green), as well as negatively charged Asp61 and Asp65 residues. Negatively charged oxygen atoms are shown in red, and the positively charged nitrogen atom of Lys105 is shown in blue.

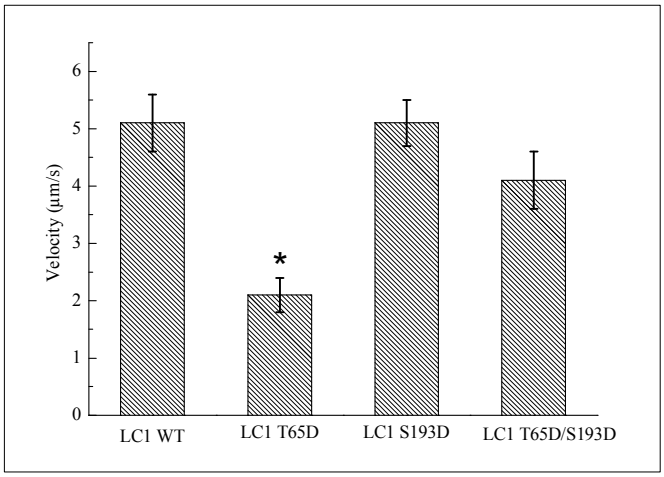
Velocity (μm/s)
0
1
2
3
4
5
6
*
LC1 WT
LC1 T65D
LC1 S193D
LC1 T65D/S193D

Fig. 1

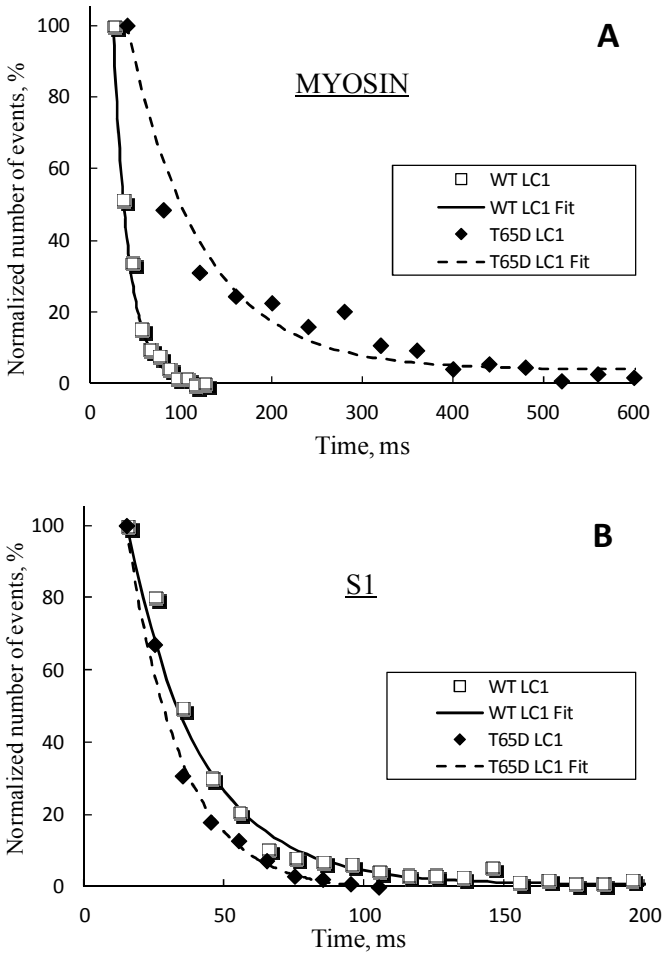
A
MYOSIN
Normalized number of events, %
Time, ms
WT LC1
WT LC1 Fit
T65D LC1
T65D LC1 Fit
B
S1
Normalized number of events, %
Time, ms
WT LC1
WT LC1 Fit
T65D LC1
T65D LC1 Fit

Fig. 2

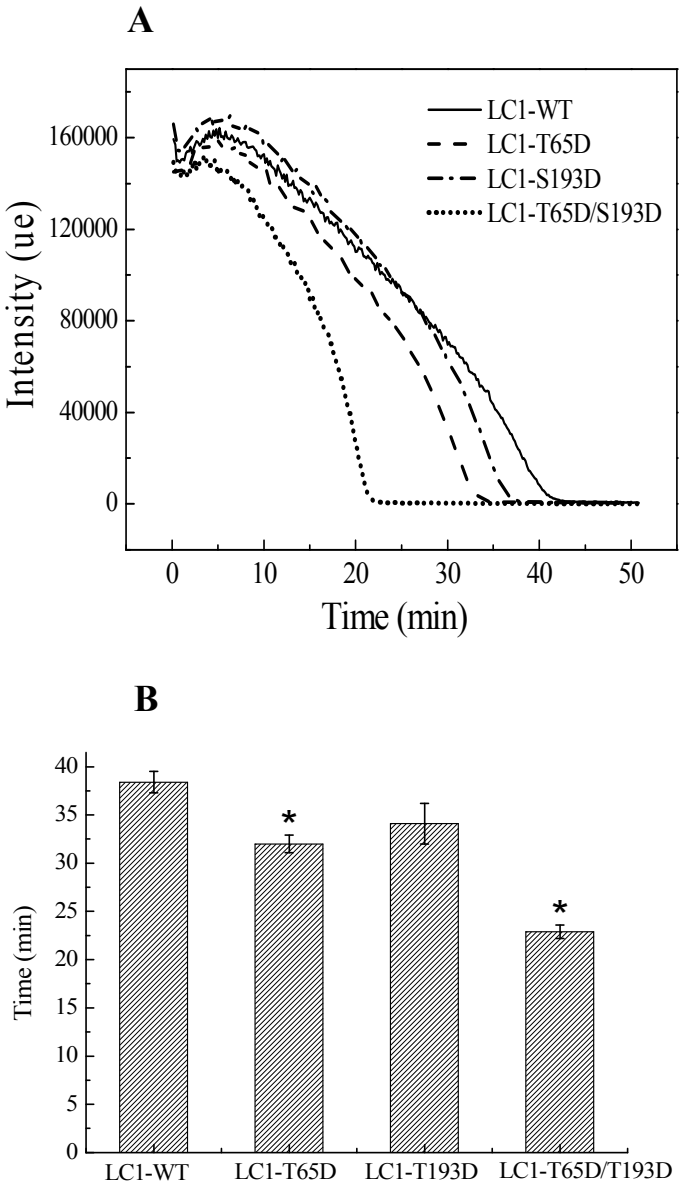
A
LC1-WT
LC1-T65D
LC1-S193D
LC1-T65D/S193D
Intensity (ue)
160000
120000
80000
40000
0
0
10
20
30
40
50
Time (min)
B
Time (min)
40
35
30
25
20
15
10
5
0
*
*
LC1-WT
LC1-T65D
LC1-T193D
LC1-T65D/T193D

Fig. 3

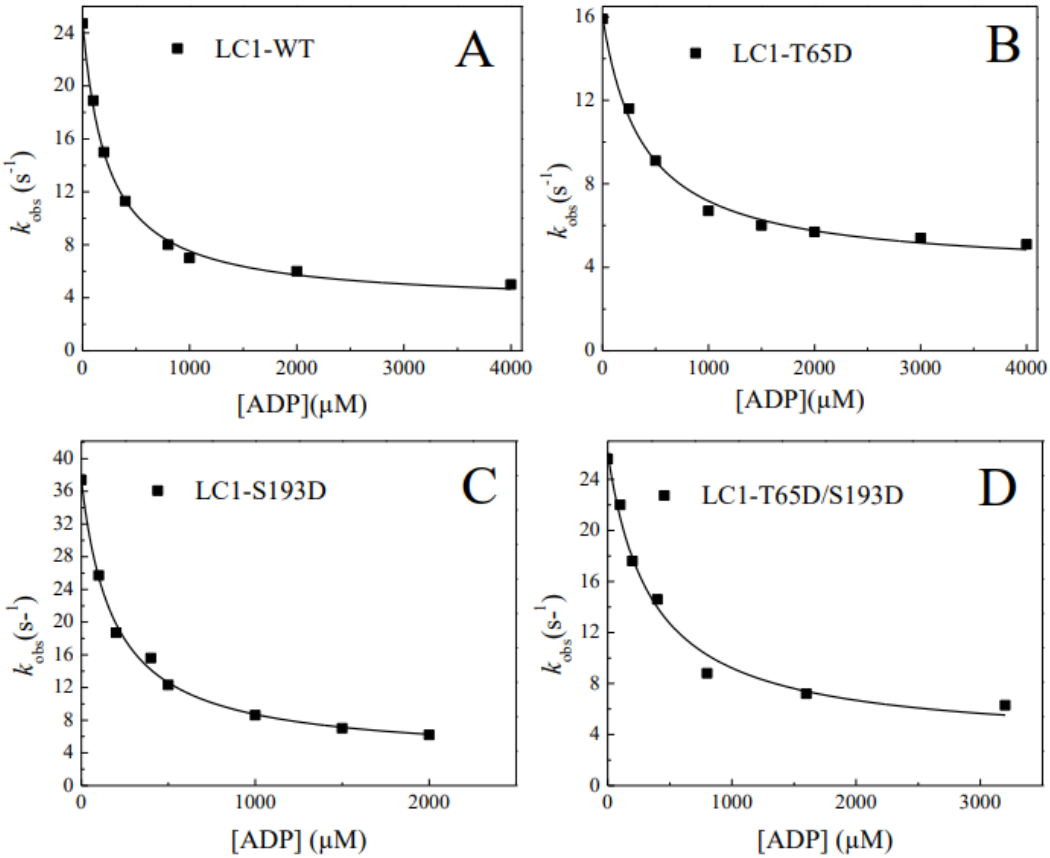
LC1-WT
A
k_{obs} (s^{-1})
[ADP](μM)
LC1-T65D
B
k_{obs} (s^{-1})
[ADP](μM)
LC1-S193D
C
k_{obs} (s^{-1})
[ADP] (μM)
LC1-T65D/S193D
D
k_{obs} (s^{-1})
[ADP] (μM)

Fig. 4

```
LC1_skel_RABBIT      61-DRTG-DSKITLS-71
LC1_skel_HUMAN       63-DRTG--DSKITLS-73
LC1_vent_HUMAN       62-DRTPKCEMKITYG-76
                        ***   : *** .
```

Fig. 5

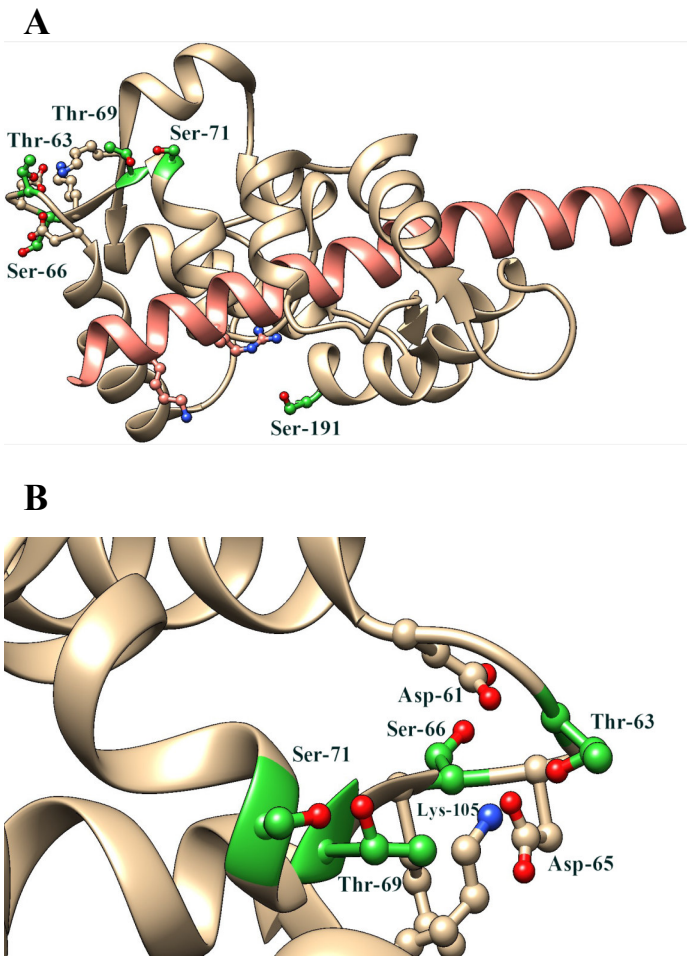

Fig. 6